Dual Action of NAMI-A in Inhibition of Solid Tumor Metastasis: Selective Targeting of Metastatic Cells and Binding to Collagen[1]

Gianni Sava,[2] Sonia Zorzet, Claudia Turrin, Francesca Vita, MariaRosa Soranzo, Giuliano Zabucchi, Moreno Cocchietto, Alberta Bergamo, Stefano DiGiovine, Gabriella Pezzoni, Luigi Sartor, and Spiridione Garbisa

Foundation Callerio-Onlus, Trieste [G. S., C. T., F. V., M. C., A. B.]; Departments of Biomedical Sciences [G. S., S. Z.] and Physiology and Pathology [F. V., M. S., G. Z.], University of Trieste, Trieste; Novuspharma, Milano [S. D., G. P.]; and Department of Experimental Biomedical Sciences, University of Padova, Padova [L. S., S. G.], Italy

ABSTRACT

NAMI-A is a ruthenium complex endowed with a selective effect on lung metastases of solid metastasizing tumors. The aim of this study is to provide evidence that NAMI-A's effect is based on the selective sensitivity of the metastasis cell, as compared with other tumor cells, and to show that lungs represent a privileged site for the antimetastatic effects. The transplantation of Lewis lung carcinoma cells, harvested from the primary tumor of mice treated with 35 mg/kg/day NAMI-A for six consecutive days, a dose active on metastases, shows no change in primary tumor take and growth but a significant reduction in formation of spontaneous lung metastases. Transmission electron microscopy examination of lungs and kidney shows NAMI-A to selectively bind collagen of the lung extracellular matrix and also type IV collagen of the basement membrane of kidney glomeruli. The half lifetime of NAMI-A elimination from the lungs is longer than for liver, kidney, and primary tumor. NAMI-A bound to collagen is active on tumor cells as shown *in vitro* by an invasion test, using a modified Boyden chamber and Matrigel, and it inhibits the matrix metallo-proteinases MMP-2 and MMP-9 at micromolar concentrations, as shown *in vitro* by a zimography test. These data show NAMI-A to significantly affect tumor cells with metastatic ability. Binding to collagen allows NAMI-A to exert its selective activity on metastatic cells during dissemination and particularly in the lungs. These data also stress the wide spectrum of daily doses and treatment schedules at which NAMI-A is active against metastases.

INTRODUCTION

The possibility of identifying a new anticancer drug among ruthenium complexes has drawn the attention of several researchers (1–3). These studies focused on the mode of binding to DNA and the advantages provided by the ruthenium ions for this action (4). The compound NAMI-A, namely imidazolium *trans*-imidazoledimethylsulfoxidetetrachlororuthenate, is an indirect outcome of this effort (5). Even so, the compound was abandoned as a conventional chemotherapeutic agent in favor of its development as a selective antimetastatic compound (6).

NAMI-A has repeatedly been shown to inhibit metastasis formation through a mechanism unrelated to conventional cell cytotoxicity (7, 8). Experimental evidence confirms NAMI-A as one of the new agents effective on specific determinants of tumor malignancy, such as angiogenesis, matrix metalloproteinases, and mitogen-activated pathways (9–11). However, data available do not explain which of these determinants is the primary target of the activity of NAMI-A. Nor can we say whether the effects reported are secondary to other types of interaction, because of the complex molecular biological network that links these three determinants and significant influences that may derive from disturbance of any of the steps of tumor malignancy (12–17).

In fact, NAMI-A shows metastasis inhibition in all of the experimental models of solid tumor under test, and metastases are inhibited independently of their stage of growth and despite the effectiveness at primary tumor site (18, 19). NAMI-A is active on lung metastases also when it is dosed by the p.o. route (20). Although the *in vitro* effects of NAMI-A on tumor invasion and angiogenesis may explain the *in vivo* effects of this compound on the extracellular matrix at primary tumor site (21), nothing can be said as yet to substantiate the efficacy of NAMI-A on advanced lung metastases in mice with late treatments (18) or treated after surgical removal of the primary tumor.[3]

We therefore studied the interactions of NAMI-A with lung tissue components and primary tumor cells to help clarify the mechanisms of metastasis inhibition. In particular, we investigated the change of malignancy of tumor cells, after *in vivo* exposure to NAMI-A, by repeated passages in healthy untreated mice, the inhibition of Matrigel invasion of tumor cells briefly exposed to NAMI-A, and the ultrastructural distribution of NAMI-A in lung and kidney by TEM.[4]

Received 10/16/02; revised 1/20/03; accepted 1/22/03.
The costs of publication of this article were defrayed in part by the payment of page charges. This article must therefore be hereby marked *advertisement* in accordance with 18 U.S.C. Section 1734 solely to indicate this fact.
[1] Supported with contributions from the Associazione Italiana per la Ricerca sul Cancro, Ministry of Education and Research, in the framework of the project pharmacological mechanisms of the antimetastatic activity of metal-based drugs, Laboratory for Investigating New Antimetastasis Drugs laboratory, and within the European Co-operation in the Field of Scientific and Technical Research D20/00005/01 Project.
[2] To whom requests for reprints should be addressed, at Fnd Callerio-Onlus, via A. Fleming 22-31, 34127 Trieste, Italy. Phone and Fax: 39 (040) 569934; E-mail: gsava@fcmail.univ.trieste.it.

[3] G. Sava, unpublished data.
[4] The abbreviations used are: TEM, transmission electron microscopy; FBS, fetal bovine serum; SCID, severe combined immunodeficiency; NCI, National Cancer Institute.

MATERIALS AND METHODS

Compound and Treatment. Imidazolium *trans*-imidazoledimethylsulfoxide-tetrachlororuthenate, ImH[*trans*-$RuCl_4$-(DMSO)Im] (NAMI-A), was prepared according to already reported procedures (5).

Cell Cultures. The TS/A adenocarcinoma cell line was kindly supplied by the group of G. Forni (Consiglio Nazionale delle Ricerche Centro di Immunogenetica ed Oncologia Sperimentale, Torino, Italy). Vials of the original line were held in liquid N_2. The cell line was maintained in RPMI 1640 (Sigma Chemical Co., St. Louis, MO) supplemented with 10% FBS (HyClone Europe, Milan, Italy), 2 mM L-glutamine (HyClone Europe), and 50 μg/ml Gentamicin Sulfate solution (Irvine Scientific, Santa Anna, CA). For experimental purposes, the cells were sown directly onto plastic plates.

Proliferation Assays. TS/A cells were plated in 6-well plates at day 0 and treated at day 1 with 1, 10, and 100 μM NAMI-A in complete medium for 1, 16, or 72 h. In this latter case, the treatment was applied once for 72 h or renewed daily. At the end of drug challenge, cells were collected by centrifugation, and total cells recovered were counted using the trypan blue exclusion test.

Invasive Potential of TS/A Cells. Invasive ability was measured in a transwell cell culture chamber (Costar, Milan, Italy) according to the method of Albini *et al.* (22); the bottom surface of a polyvinylpyrrolidone-free polycarbonate filter (6.5-mm diameter and 8-μm pore size) was coated with 30 μg/50 μl Matrigel (Becton Dickinson, Bedford, MA) and air dried overnight at room temperature. The filters were reconstituted with RPMI 1640 immediately before use. TS/A adenocarcinoma cell line, pretreated for 1 h with NAMI-A (0.1 mM in PBS), was treated with trypsine, collected by centrifugation, resuspended in RPMI 1640 supplemented with 10% FBS, and sown in triplicate in the top compartment chamber (1×10^5 cells/100 μl). The bottom compartment was filled with RPMI 1640 supplemented with 10% FBS, 2 mM L-glutamine, and 50 μg/ml Gentamicin Sulfate solution. Invasion was scored after 72 or 96 h of incubation in a humidified CO_2 incubator at 37°C. After incubation, the filters were fixed with methanol (−20°C) and stained with H&E. The cells on the top surface of the filter were removed using a cotton swab. Tumor cells that had migrated from the top to the bottom side of the filter were counted by light microscopy at 400 magnification. The invasion was expressed as a percentage of total invasion compared with the original number of cells sown on day 0, calculated by the following formula: [Total number of invading cells (bottom well sample)]/[Total number of sown cells (top well sample)] × 100. For each experiment, cells in ≥3 wells were counted.

MMP-2 and MMP-9 Gelatin-Zymography and Activity. To visualize the direct effect of NAMI-A on enzymes MMP-2 and MMP-9, SDS-PAGE gelatin-zymography was carried out using gelatinase-containing medium conditioned by neuroblastoma SK-N-BE and fibrosarcoma HT-1080 cells. At the end of electrophoresis, the gels were cut into strips and incubated with different concentrations of NAMI-A (0–6 mM) for 30 min at 4°C and then for 18 h at 37°C. EDTA 10 mM was used as negative control. The gel strips were then stained with 0.5% Coomassie brilliant blue. The gelatinolytic regions were observed as white bands against a blue background. MMP activity was measured by scoring the intensity of bands by computerized image analysis (Apple Computer, Inc., Cupertino, CA).

***In Vivo* Effects on Solid Tumors.** Lewis lung carcinoma was grown in BD2F1 female mice purchased from Harlan-Nossan (San Pietro al Natisone, Italy). The Lewis lung carcinoma line used was originally obtained from the Tumor Depository Bank, NCI, NIH (Bethesda, MD), and was locally maintained in C57Bl/6 mice by serially biweekly passages according to relevant NCI protocols: 10^6 tumor cells of a single cell suspension, prepared by mincing with scissors the primary tumors from donors similarly implanted 2 weeks previously, were injected i.m. into the left hind calf of experimental groups. The minced tissue was filtered through a double layer of sterile gauze, centrifuged at 200 × *g* for 10 min, and resuspended in an equal volume of PBS; viable cells were counted by the trypan blue exclusion test.

MCa mammary carcinoma was grown in female CBA mice purchased from Harlan-Nossan. The line of MCa mammary carcinoma used was originally obtained from the Department of Biology, Rudjer Boskovich Institute of Zagreb, Croatia. The procedures for tumor graft and transplantation were those used for Lewis lung carcinoma.

For both Lewis lung carcinoma and MCa mammary carcinoma, primary tumor growth was measured using calipers to determine two orthogonal axes; tumor volume is given by the formula: $(\pi/6) \times a^2 \times b$, where *a* is the shorter axis, and *b* is the longer axis, assuming tumor density equal to 1. Lung metastases were counted by examining lung surface immediately after killing of the animals by cervical dislocation. Lungs were dissected into the five lobes (lobus sinister, lobus cranialis dexter, lobus medius dexter, lobus caudalis dexter, and lobus accessorius), washed with PBS, and examined under a low-power microscope equipped with a calibrated grid. The weight of each metastasis was calculated by applying the same formula used for primary tumors; the sum of individual weights gives the total weight of metastatic tumor per animal.

The human lung cancer cell line H460M2, selected for its high lung colonization potential, was provided by the NCI of Milan (G. Pratesi). The tumor cell line is routinely cultured in RPMI 1640 (Bio-Whittaker Europe, Parc Industriel de Petit Rechain, Belgium) supplemented with 10% FBS (Life Technologies, Inc., Invitrogen, San Giuliano Milanese, Italy), 2% HEPES buffer, and 1% 200 mM L-glutamine (Bio-Whittaker Europe) at 37°C in a humidified atmosphere of 5% CO_2 in air. Tumor cells (3×10^6 in 50 μl of PBS) were injected into the footpad of 5-week-old male SCID CB.17 mice (20–22 grams; Harlan, Correzzana MI, Italy), and the primary tumor was surgically removed on day 22 after inoculum; the mass was ~600 mg, as determined by caliper measurement. Before surgery, mice were anesthetized by s.c. administration of an anesthetic mixture (10 ml/kg bodyweight) containing 13.6 mg/kg b.w. Ketamine (Ketavet, Parke-Davis) and 17 mg/kg b.w. Xylazine (Rompun, Bayer AG).

After skin incision and removal up to the pelvic region, the visible femoral artery and vein were ligated. The primary tumor of the hind footpad and popliteal lymph nodes were resected by amputation of the extremity (above knee amputation). After

renewed disinfection of the surgical area, the lips of the wound were carefully brought together (skin edge approximation) to cover the amputation stump fully. Finally, the incision was closed using two wound clamps. The number and size of lung metastases on the entire lung surface were determined by morphometric analysis of the lung lobes using image analysis software. The fixed lungs were cleaned from connective tissue and split into five separate lobes. Two digital pictures of the five lobes arranged on a glass plate were then taken from above and below. Using Image Plus 4.0 (Media Cybernetics, Silver Spring, MD) software, the average diameter of each metastasis was marked manually. Assuming that metastases grow roughly spherical, the volume of each metastasis was calculated using the formula: $V = (\pi/6) \times \text{diameter}^3$.

TEM Analysis. Specimens of lung and kidney were processed for ultrastructure studies. Tissue blocks were promptly fixed in a solution of 3% glutaraldehyde (Serva, Heidelberg, Germany) in 0.1 M cacodylate buffer (pH 7.3) for 3 h at 4°C, rinsed three times (10 min each wash) in the same buffer, and postfixed in 1% OsO_4 for 1 h at 4°C. The samples were then dehydrated in graded ethanols and embedded in Dow Epoxy Resin 332 (23). Ultrathin sections were cut using an ultratome Leica Ultracut UCT8 (Leica, Mikrosysteme Aktiengesellschaft, Wien, Austria), double stained with uranyl acetate and lead citrate (24), and examined with a Phillips EM 208 transmission electron microscope.

Atomic Absorption Spectroscopy. A small portion of each specimen was weighed and dried overnight at 80°C and completed at 105°C in Nalgene cryovials. Tissue decomposition was facilitated by the addition of an aliquot of tetramethylammoniumhydroxide (25% in water; Aldrich Chimica, Gallarate, Milano, Italy) and milliQ water at a ratio of 1:1 directly in each vial at room temperature and under shaking (modified from Ref. 25). The final volumes were adjusted to 1 ml with milliQ water. The concentration of ruthenium was measured in triplicate using a Graphite Furnace Atomic Absorption Spectrometer, model SpectrAA-300, supplied with a specific ruthenium emission lamp (hollow cathode lamp P/N 56–101447-00; Varian, Mulgrave, Victoria, Australia). To correct for possible deterioration of the graphite furnace during a daily working session, a reslope standard was measured every six samples. Changes in the readings of this standard are included in the calculation of the NAMI-A concentration of the samples. If the values of two subsequent reslope readings deviated by >20%, then the graphite furnace was replaced. The lower and higher limits of quantitation were set at the levels corresponding to the lower and higher standard concentrations, respectively. The limit of detection was estimated according to the EURACHEM guide, "the fitness for purpose of analytical methods." Lower limit quantitation, higher limit quantitation, and limit of detection were, respectively: 12.5, 200, and ~10 ng $\times$ Ru $\times$ ml^{-1} of sample. The quantification of ruthenium was carried out in 10-μl samples at 349.9 nm with an atomizing temperature of 2500°C, using argon as carrier gas at a flow rate of 3 l min^{-1}. Additional details concerning the furnace parameter settings are reported in Cocchietto *et al.* (26). Before each daily analysis session, a five-point calibration curve was obtained using Ruthenium Custom-Grade Standard 998 μg ml^{-1} (Inorganic Ventures, Inc., St. Louis, MO).

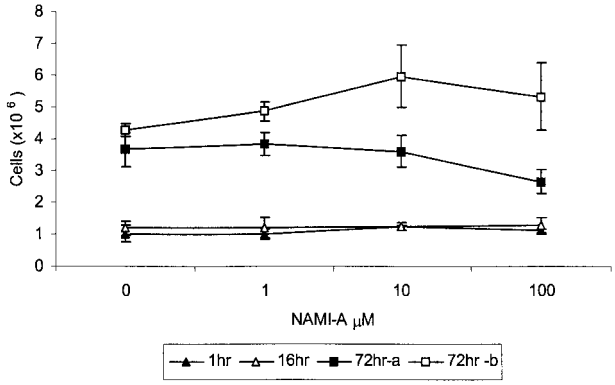

Fig. 1 Effects of NAMI-A on TS/A cell proliferation. Cells were sown on day 0 and treated on day 1 with 0, 1, 10, and 100 μM NAMI-A dissolved in complete medium for 1, 16, or 72 h. The samples denoted 72 h-a received the drug once for 72 h; in the samples 72 h-b, the drug was changed daily. Cell number was evaluated by trypan blue exclusion test at the end of treatment.

Animal Studies. Animal studies were carried out according to guidelines in force in Italy (DDL 116 of 21/2/1992 and subsequent addenda) and in compliance with the Guide for the Care and Use of Laboratory Animals (Department of Health and Human Services Publ. No. 86-23, Bethesda, MD, NIH, 1985).

Statistical Analysis. Experimental data were subjected to computer-assisted statistical analysis using ANOVA, Tukey-Kramer post-test, and nonparametric Mann-Whitney test. Differences of $P < 0.05$ were considered to be significantly different from controls.

RESULTS

Cytotoxic Effects on TS/A Adenocarcinoma Cells. The effects of NAMI-A on the viability of TS/A cells, measured by variation of the number of cells recovered from multiwell plates after 1-, 16-, or 72-h treatment, are reported in Fig. 1. No significant modification was observed on these cells over these treatment periods, as determined by the count of cells harvested from the plates. In particular, no change of cell proliferation occurred after treatment of TS/A cells with 0.1 mM NAMI-A for 72 h, either when the compound was left with these cells for the whole period or when the incubation medium, containing NAMI-A, was changed every day of the 3-day treatment.

Effects on Matrigel Invasion of TS/A Adenocarcinoma Cells. The cells, treated *in vitro* with 0.1 mM NAMI-A for 1 h, showed a reduced capacity to invade and migrate through a Matrigel barrier in the Boyden chamber. The evaluation of cell invasion, performed at 96 h (Fig. 2), showed significantly fewer cells on the opposite site of the chamber, the amount being dose dependent and ~35–40% of untreated controls at 80 and 120 μM NAMI-A concentrations.

The effects of NAMI-A on tumor cell invasion were also studied in a system in which cells were layered on Matrigel before exposure to NAMI-A or in another system in which Matrigel itself was exposed to NAMI-A before cells were layered on it. Under all these conditions, NAMI-A proved to be active in inhibiting Matrigel crossing when the treated tumor

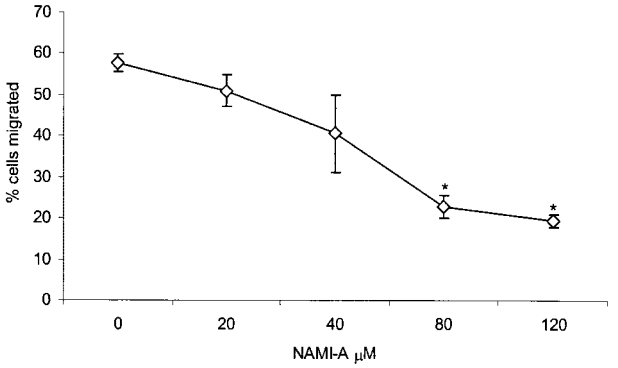

Fig. 2 Effect of NAMI-A on invasion of TS/A adenocarcinoma cells through Matrigel-coated polycarbonate filters. TS/A cells, treated previously with NAMI-A at 0–120 μM for 1 h in PBS Ca^{2+}-Mg^{2+}, were sown on the top compartment of a 24-well transwell chamber, coated with Matrigel (30 μg/50 μl). Data represent cells that had completely passed through the Matrigel-coated barrier after 96 h and are located in the bottom compartment of the transwells. Data are expressed as percentage ± SE of invading cells relative to the corresponding controls. Statistical analysis: ANOVA and Tukey-Kramer post-test (*$P < 0.05$; **$P < 0.01$, *versus* controls).

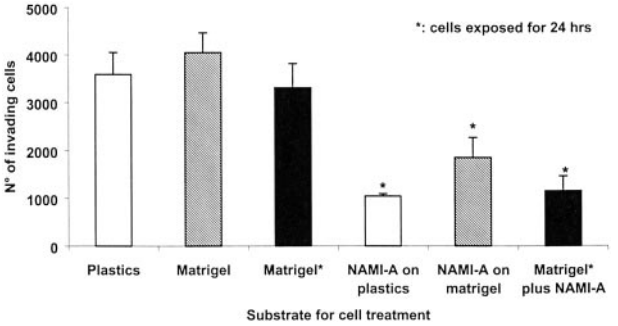

Fig. 3 *In vitro* invasion by TS/A cells through Matrigel-coated polycarbonate filters. TS/A cells, exposed previously to NAMI-A, were sown on the top compartment of a 24-well transwell chamber, coated with Matrigel (30 μg/50 μl). The treatments performed are: (*a*) 10^{-4} M NAMI-A for 1 h on cells layered previously and grown for 24 h in intact 6-well plastic plates (Plastics); (*b*) 10^{-4} M NAMI-A for 1 h on cells layered previously and grown for 24 h in 6-well plastic plates coated previously with 240 μg/400 μl Matrigel; and (*c*) TS/A cells grown in contact for 24 h with 240 μg/400 μl Matrigel preexposed for 1 h to 10^{-4} M NAMI-A on 6-well plastic plates. Data represent cells that had completely passed through the Matrigel-coated barrier after 72 h and are located in the bottom compartment of the transwells. Data are expressed as percentage ± SE of invading cells relative to the corresponding controls. Statistical analysis: ANOVA and Tukey-Kramer post-test (*$P < 0.05$; **$P < 0.01$, *versus* controls).

cells were placed on the top side of a Boyden chamber coated previously with Matrigel. Inhibition of Matrigel invasion was determined as the spontaneous crossing of this barrier by tumor cells after a 72-h incubation in the absence of any chemoattractant put in the bottom chamber (Fig. 3). However, it is known that the use of conditioned medium of NIH 3T3 cells, to study the effects of NAMI-A on chemotaxis, does not interfere with the overall result (9).

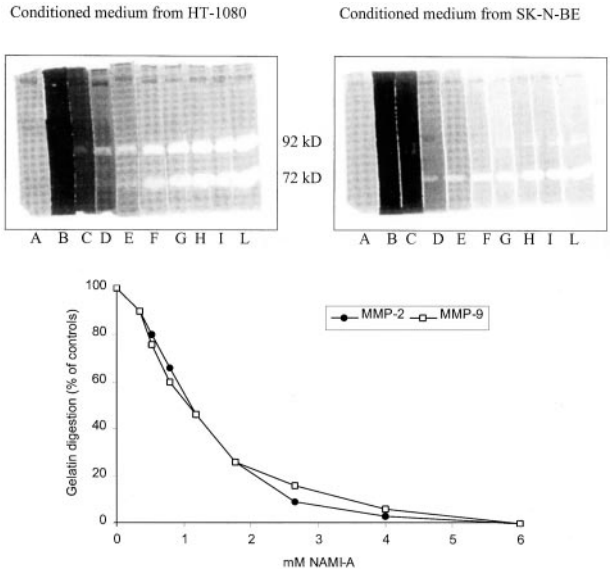

Fig. 4 Direct effect of NAMI-A on MMP-2 (M_r 72,000) and MMP-9 (M_r 92,000) gelatinases. MMP-2 activity was evaluated from a densitometric scan of bands appearing on a SDS/polyacrylamide/gelatin gel loaded with culture medium of human SK-N-BE neuroblastoma and HT-1080 fibrosarcoma cells and treated with increasing concentrations of NAMI-A ranging from 0 to 6 mM. As negative control, 10 mM EDTA were used. Lane identification: *A*, 10 mM EDTA; *B*, 6 mM; *C*, 4 mM; *D*, 2.66 mM; *E*, 1.77 mM; *F*, 1.18 mM; *G*, 0.79 [*0.79] mM; *H*, 0.52; *I*, 0.35 mM; *L*, 0 mM NAMI-A. *Lanes D, C,* and *B* are progressively darker because of NAMI-A stain. The densitometric values are plotted on the graph.

Effect on MMP-2 and MMP-9 Activity. The study of the direct effects of NAMI-A on MMP-2 and MMP-9 was performed using gelatin-zymography test. Both gelatinases, obtained from the culture medium conditioned by human fibrosarcoma (HT-1080) and neuroblastoma (SK-N-BE) cell lines, were challenged overnight with increasing concentrations of NAMI-A in the presence of their substrate. Fig. 4 shows that fibrosarcoma cells secreted overlapping amounts of MMP-2 and MMP-9, whose activity declined in step with increasing NAMI-A concentrations. The residual amount of enzymatic activity is plotted separately. Similar results were obtained with the neuroblastoma-conditioned medium, where MMP-2 represented ~80% of the secreted gelatinases.

Effects on Tumor Growth and Metastasis Formation. The effects of NAMI-A on primary tumor growth and formation of lung metastases were studied at various doses and treatment schedules. In particular, single doses of 193 (corresponding to the LD_{10}), 137, and 95 mg/kg and repeated treatments with 2-, 1-, or 0-day free intervals between two subsequent administrations were used. Repeated treatments were calculated to always give the same total amount of NAMI-A, *i.e.,* 210 mg/kg. NAMI-A reduced primary tumor growth only at the single dose of 137 mg/kg; the top dose of 193 mg/kg is toxic to mice, and the effect on primary tumor is less evident (Fig. 5, *top*). Conversely, all of the treatment schedules applied significantly reduced the formation of lung metastases; no statistically significant difference was measured among the different treatments (Fig. 5, *bottom*).

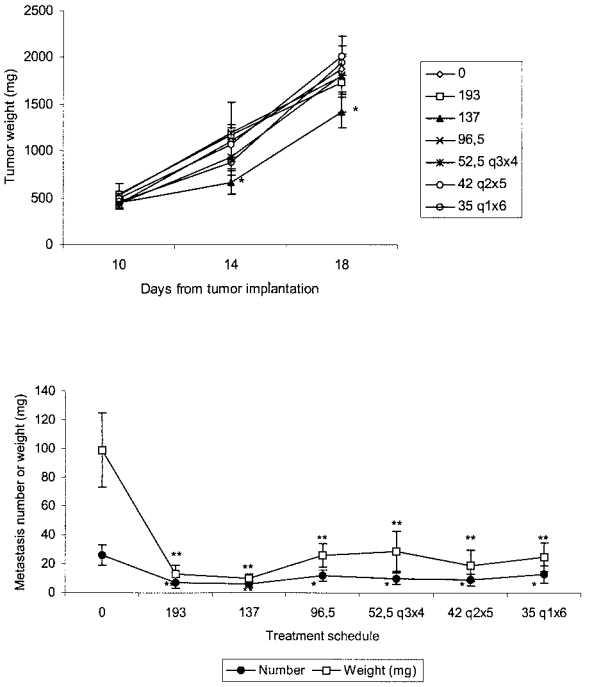

Fig. 5 Metastasis reduction by different schedules of NAMI-A. Groups of 10 CBA mice, implanted i.m. with 10^6 MCa mammary carcinoma cells on day 0, were given single i.p. injections of 96.5, 137, or 193 mg/kg NAMI-A on day 10 or repeated treatments of 35, 42, or 52.5 mg/kg/day, respectively, once per day on days 10–15 (q1 × 6), at 48-h intervals on days 10–18 (q2 × 5), or at 72-h intervals on days 10–19 (q3 × 4). Lung metastases were counted on day 23. Statistical analysis: ANOVA and Tukey-Kramer post-test (*$P < 0.05$; **$P < 0.01$, *versus* controls).

Effects on Tumor Metastatic Potential. The transplantation of Lewis lung carcinoma cells, harvested from the primary tumor of mice treated i.p. with the repeated dose of 35 mg/kg/day given for six consecutive days, shows a marked and statistically significant reduction of lung metastasis growth for two subsequent transplant generations in which animals were not further treated (Table 1). Metastasis reduction is not associated to the reduction of primary tumor, which is not statistically different from that of untreated controls.

TEM Examination of Lung and Kidney. Ruthenium is an electron dense atom and visible as black spots under electron microscopy examination. NAMI-A clearly lies along the collagen fibers of the lung; no other extracellular matrix constituent, in particular, elastin, also largely distributed in the lung, shows the black spots of ruthenium, which labels the lung collagen fibers (Fig. 6, *b–d*). NAMI-A is particularly abundant around the metastatic foci whose collagen-rich regions are clearly electron dense (Fig. 6*d*).

NAMI-A also binds to the type IV collagen typical of basement membranes. Fig. 7, *a* and *b* shows the basement membrane of glomeruli in the kidney. This basement membrane, present as a double parallel line attached to the wall of the endothelial cell, is rich in type IV collagen and clearly colored black in mice treated with NAMI-A (Fig. 7*b*).

Table 1 Effects of NAMI-A on the metastatic potential of Lewis lung carcinoma

Transplant generation	Primary tumor[a]	Lung metastases[b]	
		No.	Weight
0	71.7 ± 10.7	45.5 ± 12.1[c]	32.9 ± 8.5[c]
1	70.5 ± 9.8	41.7 ± 13.5[c]	30.0 ± 10.4[c]
2	90.9 ± 5.4	68.2 ± 13.2	44.6 ± 5.3[c]
3	65.2 ± 11.7	41.9 ± 11.5[c]	37.2 ± 7.6[c]

[a] Measured on day 15.
[b] Measured on day 21.
[c] $P < 0.05$ from untreated controls, Student-Newmann-Keuls ANOVA. Groups of 10 BD2F1 hybrids, inoculated i.m. into the left hind calf with 10^6 cells of Lewis lung carcinoma on day 0, were given i.p. NAMI-A at 35 mg/kg/day on days 10–14 (generation 0). Generation 1 was obtained by similar inoculations of tumor cells harvested from these two groups; generations 2 and 3 were run subsequently. Each value is the mean ± SE of the percentage ratio between treated and relevant control groups for each transplant generation. The actual values in a representative control group was 1109 ± 173 mg (primary tumor), 26 ± 7 number, and 99 ± 26 mg of weight of metastases per animal.

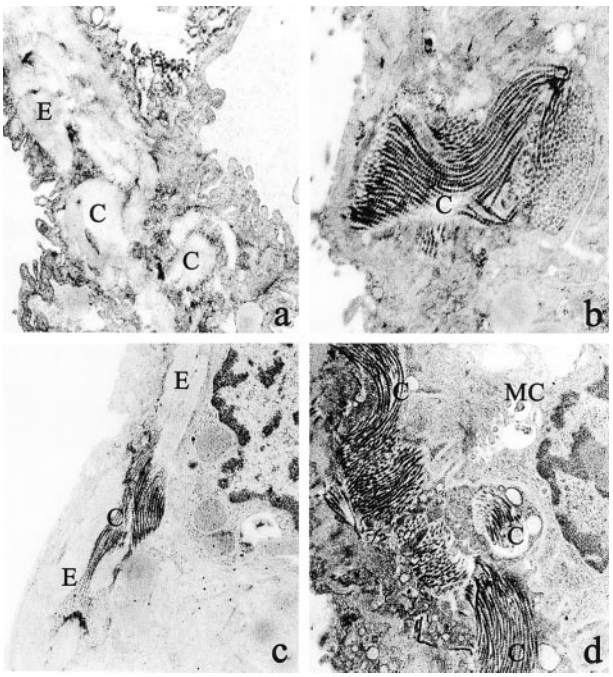

Fig. 6 *a–d*, ultrastructural appearance of NAMI-A binding to fibrillar lung collagen. *C*, collagen; *E*, elastin; *MC*, metastatic cell.

Half Lifetime of Elimination by Host Organs. The measurement of the elimination rate of NAMI-A from primary tumor, liver, kidney, and lung was measured by atomic absorption spectroscopy in samples obtained from mice with Lewis lung carcinoma and treated i.p. for six consecutive days with 35 mg/kg/day NAMI-A. Samples were collected from 24 to 144 h after final administration. NAMI-A is eliminated from the lungs at a rate markedly slower than that from any other organ tested, the half lifetime being ~180 h; for comparison, the release of compound from the primary tumor is significantly faster, the

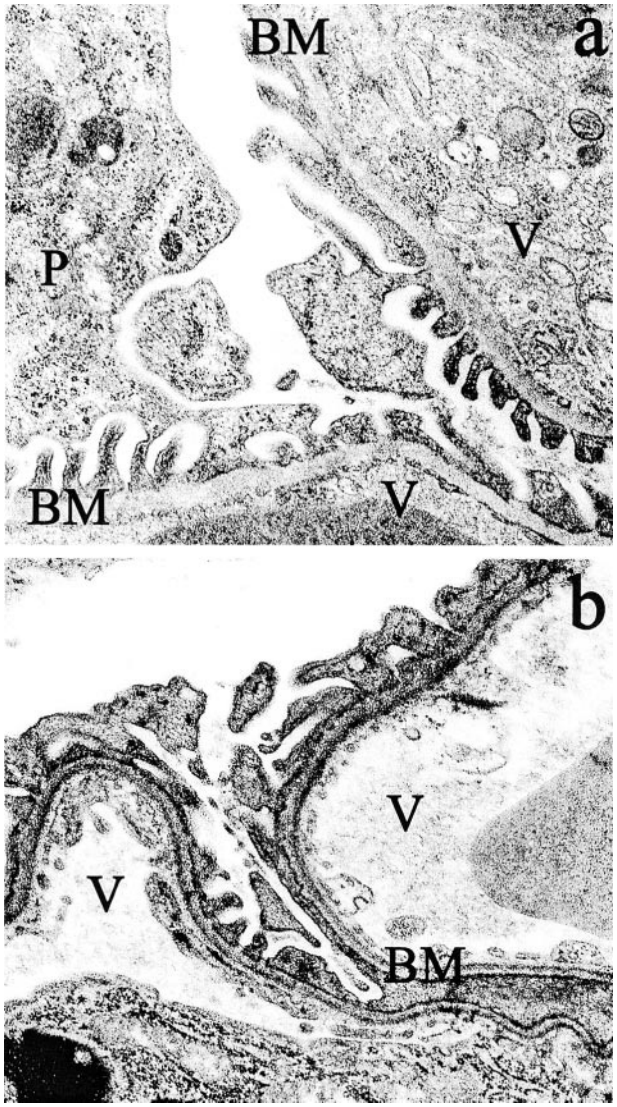

Fig. 7 *a* and *b*, ultrastructural appearance of NAMI-A binding to type IV collagen on basal membrane of kidney glomerulus. *P*, collagen; *V*, glomerulus blood vessel; *MB*, basal membrane.

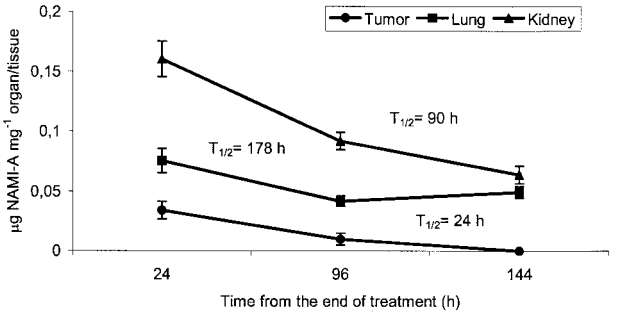

Fig. 8 $T_{1/2}$ of elimination of NAMI-A from liver, kidney, primary tumor, and lungs of mice bearing MCa mammary carcinoma and treated with doses of NAMI-A active on lung metastases. $T_{1/2}$ was calculated according to the formula $0.693/K_e$, where K_e is the constant of elimination and obtained by linear interpolation of the ln of NAMI-A concentration *versus* time. Because the linear interpolation was carried out on three experimental times, the estimated $T_{1/2}$ should be considered as indicative; in any case, the R^2 values lay close to 0.9.

period being equivalent to ~24 h (Fig. 8). From these data, it is possible to estimate that a week after treatment, the concentration of NAMI-A in the lungs still exceeds 10^{-4} M.

DISCUSSION

NAMI-A has repeatedly been described to inhibit lung metastasis growth of solid metastasizing tumors (7, 19, 21). This present study confirms the selective effect on metastases of this ruthenium-derived compound, compared with the reduction effects of primary tumor growth, over many dosages, including acute treatment of advanced tumors.

Metastases are reduced because NAMI-A acts primarily on tumor cells endowed with metastatic ability. The marked reduction of metastatic capacity of tumor cell suspensions, prepared from primary tumors obtained from mice treated with NAMI-A, indicates that cells endowed with metastatic ability are effectively removed from these suspensions; our study shows that this effect is maintained for two transplant generations free of treatment. This effect seems not to be attributable to chemical xenogenization of tumor cells (27, 28), unless we consider that only metastatic cells undergo this epigenetic change. Previous studies showed NAMI, the precursor of NAMI-A, to progressively reduce to zero the metastatic ability of primary tumors repeatedly treated for up to seven transplant generations with no appreciable modification of primary tumor growth (29). It thus appears that NAMI-A modifies the heterogeneity of tumor cell population in the primary tumor by eliminating those with the highest metastatic ability. The removal of only the metastatic cells from the primary tumor may explain the modest activity of NAMI-A at primary tumor level, where these cells often represent a small fraction (30), considering that also host-infiltrating cells appear to be resistant to NAMI-A cytotoxicity (31).

Metastases thus appear to be a privileged target for NAMI-A, a conclusion supported by the particular efficacy of this compound in the lung, where the tumors tested usually metastasize. NAMI-A reaches a significant concentration in the lung and has a favorable half lifetime of elimination about five times longer than that from the primary tumor. The slow release of NAMI-A from the lung is attributed to its binding to extracellular matrix collagen, as demonstrated by electron microscopy examination. We believe that the *in vitro* test on invasion, using Matrigel pretreated with NAMI-A, demonstrates that NAMI-A, once bound to collagen, maintains its pharmacological activity on metastases. The increased deposition of fibrillar collagen around metastases and the binding of NAMI-A to this collagen allow speculation on the high possibility of a metastatic tumor cell being affected by NAMI-A in the lungs as compared with the primary tumor. Moreover, if metastatic cells are a target for NAMI-A in preference to any other primary tumor cell, we must emphasize that only these cells are present in the lung, because metastases have a clonal origin (30). Thus, the reduction of lung metastases, significantly higher than that of the primary tumor, is the logical consequence and commonly found in mice with solid metastasizing tumors.

Table 2 *In vivo* effects of NAMI-A on the human lung H460M2 cancer cell line[a]

Treatment group	CBW%[b]	Primary tumor weight (mg)[c]	Lung metastases[d]			
			No.	% Inh.[e]	Weight (mg)	% Inh.
Treatment before surgical removal of primary tumor						
Controls	−5.2	605 (455–785)	38 (13–81)		85 (12–127)	
NAMI-A	−7.4	520 (400–635)	26 (3–92)	30	15 (1–53)	70[f]
Treatment after surgical removal of primary tumor						
Controls	−7.7		48 (9–66)		35 (7–130)	
NAMI-A	−3.6		22 (1–51)	54[g]	8 (0–46)	77[f]

[a] Groups of 15 SCID mice, implanted intrafootpad with 3×10^6 cells of H460M2 on day 0, were given i.p. on days 16–21 (presurgical treatment) or on days 23–28 (postsurgical treatment) saline (controls) or NAMI-A at 35 mg/kg/day. Surgical removal of primary tumor was performed on day 22 under general anesthesia. Each number is the median (min − max) obtained in each group.

[b] Change of body weight was calculated 50 days after tumor transplantation.

[c] Measured on day 22.

[d] Measured on day 50.

[e] Percentage inhibition *versus* controls.

[f] $P < 0.001$ *vs.* controls, Mann-Whitney test.

[g] $P < 0.05$.

The activity of NAMI-A bound to collagen also allows conclusions to be drawn on the *in vivo* effect of this compound on MMPs, because *in vitro* tests showed inhibitory activity only at micromolar concentrations. NAMI-A shows an equal propensity to bind to fibrillar type III collagen of the lung or basement membrane collagen type IV. Therefore, it is not surprising that a migrating metastatic cell, in the microenvironment in which it makes contact with the extracellular matrix (*e.g.*, the basement membrane), may find NAMI-A at relatively high (micromolar) concentration, *e.g.*, the NAMI-A concentration in the lungs at the end of an administration cycle of doses active on metastases is around 0.2–0.4 mM (Refs. 18 and 19 and present study). Measurement of the level of collagen-bound compound alone would probably reveal concentrations 5–10-fold higher in this specific microenvironment, although collagen is only a minor constituent of lung tissue. This could account for the eventual effect against MMP-2 and MMP-9; the direct inhibition of both release and activity of these gelatinases could lie behind the anti-invasive and antiangiogenic effect of NAMI-A (9, 32).

Spontaneous Matrigel invasion by tumor cells is restrained by 0.05–0.1 mM NAMI-A, concentrations that are nontoxic even after 72 h but also much lower than the IC_{50} for gelatinases (33); this evidence reinforces the idea that NAMI-A accumulation on gelatinase substrate (collagen) is crucial to the effectiveness against gelatinase activity.

The binding of NAMI-A to extracellular collagen and the consequent slow release from the lung may explain the equivalence of the antimetastatic effects for a number of different daily doses and treatment schedules used. Similarly, the peak of dose used may explain the weak effect at primary tumor site where a lower amount of collagen is present, the half lifetime is shorter, and, therefore, only a short exposure of tumor cells to NAMI-A is ensured. Provided that: (*a*) the tissue distribution of NAMI-A is not influenced by the dose administered; (*b*) the compound is rapidly removed from the peritoneal cavity (18) and quickly distributed to all organs and tissues (26); and (*c*) the rate of elimination from the tissues depends on collagen binding; then tissue concentration of NAMI-A is strictly related to the administered dose. In fact, in an experiment in which NAMI-A was given at three different doses, its lung concentration increased linearly with increases in daily dose (18, 34). Therefore, the difference between single administrations and repeated treatments is null in terms of efficacy, in that under both conditions, the goal of providing a suitable amount of NAMI-A for a time long enough to inhibit metastasis growth is reached.

Because the main toxicity detected for NAMI-A is the renal toxicity (7), which seems at least in part reversible (7, 34), it would be interesting to evaluate whether a single dose, repeated with a long drug-free interval, would provide a therapeutic index more favorable than that of the classic cycle of 6-day treatment often used. What is probably certain is that it would provide a better compliance for treating human metastases, considering that this "drug" has a greater tendency to control and stabilize the disease than to remove it with a conventional cytotoxic effect and therefore needs rather long treatment periods.

In conclusion, we demonstrate that the antimetastatic activity of NAMI-A is caused by the selectivity of action for the metastatic cell and depends on its binding to collagen, which preserves it from elimination and gives it prolonged contact with the metastatic cells in the lungs. Considering that lung metastases are common features of many human tumors, NAMI-A may represent a new and effective tool for treating them. Laboratory proof is given by the effectiveness of NAMI-A on the H460M2 human lung tumor; the i.p. treatment of the human lung tumor H460M2 xenotransplanted into the SCID mouse with 35 mg/kg/day for six consecutive days resulted in a statistically significant reduction of lung metastasis growth, independently of whether the compound was given before or after surgical removal of the primary tumor (Table 2). Data obtained with this human tumor line are in perfect agreement with the present discussion and past results, and therefore, as in the case of other treatments of mouse transplantable tumors, NAMI-A was also free of significant effects on primary tumor growth when given before surgery.

Finally, the results of the present investigation also open the way to identification of the molecular determinant/target of

NAMI-A for the selective effect on metastatic cells. These studies might allow: (*a*) prediction of the response of a given metastatic tumor to NAMI-A; and (*b*) evaluation of the chemical changes on the molecule as a key to extending this activity to metastases resistant to NAMI-A. In this context, studies in progress seem to prove the capacity of NAMI-A to specifically interfere with the mitogen-dependent signaling pathways that maintain tumor cell malignancy (10, 11).

ACKNOWLEDGMENTS

We thank Dr. E. Alessio and G. Mestroni, Department of Chemical Sciences, University of Trieste, for the preparation of the sample of NAMI-A used in the present investigation and Dr. S. Biggin for revision of the English manuscript.

REFERENCES

1. Clarke, M. J. Oncological implications of the chemistry of ruthenium. *In:* H. Sigel (ed.), Metal Ions in Biological Systems, pp. 231–283. New York: Marcel Dekker, Inc., 1980.

2. Clarke, M. J. Ruthenium complexes: potential roles in anticancer pharmaceuticals. *In:* B. K. Keppler (ed.), Metal Complexes in Cancer Chemotherapy, pp. 129–156. Weinheim, Germany: VCH, 1993.

3. Sava, G., and Bergamo, A. Ruthenium-based compounds and tumor growth control (review). Int. J. Oncol., *17:* 353–365, 2000.

4. Clarke, M. J., and Stubbs, M. Interactions of metallopharmaceuticals with DNA. *In:* A. Sigel and H. Sigel (eds.), Metal Ions in Biological Systems, pp. 727–780. New York: Marcel Dekker, Inc., 1996.

5. Mestroni, G., Alessio, E., and Sava, G. New salt of anionic complexes of Ru(III) as antimetastatic and antineoplastic agents. International Patent, PCT C 07F 15/00, A61K 31/28. WO 98/00431, 1998.

6. Sava, G., Alessio, E., Bergamo, A., and Mestroni, G. Sulphoxide ruthenium complexes: non-toxic tools for the selective treatment of solid tumour metastases. *In:* M. J. Clarke and P. J. Sadler (eds.), Topics in Biological Inorganic Chemistry, pp. 143–169. Berlin: Springer Verlag, 1999.

7. Bergamo, A., Gagliardi, R., Scarcia, V., Furlani, A., Alessio, E., Mestroni, G., and Sava, G. In vitro cell cycle arrest, *in vivo* action on solid metastasizing tumors, and host toxicity of the antimetastatic drug NAMI-A and cisplatin. J. Pharmacol. Exp. Ther., *289:* 559–564, 1999.

8. Zorzet, S., Bergamo, A., Cocchietto, M., Sorc, A., Gava, B., Alessio, E., Iengo, E., and Sava, G. Lack of *in vitro* cytotoxicity, associated to increased G_2-M cell fraction and inhibition of matrigel invasion, may predict *in vivo* selective antimetastasis activity of ruthenium complexes. J. Pharmacol. Exp. Ther., *295:* 927–933, 2000.

9. Vacca, A., Bruno, M., Boccarelli, A., Coluccia, M., Ribatti, D., Bergamo, A., Garbisa, S., Sartor, L., and Sava, G. Inhibition of endothelial cell function and of angiogenesis by the metastasis inhibitor NAMI-A. Br. J. Cancer, *86:* 993–998, 2002.

10. Sava, G., Bergamo, A., Cocchietto, M., Flaibani, A., Gava, B., Pintus, G., Sorc, A., Tadolini, B., Ventura, C., and Zorzet, S. Interaction of NAMI-A with the regulation of cell cycle progression. Clin. Cancer Res., *6:* 4566s (abstract #501), 2000.

11. Bergamo, A., Pintus, G., Tadolini, B., Posadino, A. M., Sanna, B., Debidda, M., Bennardini, F., Ventura, C., Vita, F., Soranzo, M. R., Frausin, F., Cocchietto, M., Furlani, A., Scarcia, V., and Sava, G. NAMI-A, a ruthenium based compound capable of controlling metastasis growth by interfering with cancer complexity. The Pezcoller Fnd. J., *9:* 13–14, 2001.

12. Albini, A. Tumour and endothelial cell invasion of basement membranes. Pathol. Oncol. Res., *4:* 230–241, 1998.

13. Chambers, A. F., and Matrisan, L. M. Changing views of the role of matrix metalloproteinases in metastasis. J. Natl. Cancer Inst. (Bethesda), *89:* 1260–1270, 1997.

14. Shapiro, S. D. Matrix metalloproteinase degradation of extracellular matrix: biological consequences. Curr. Opin. Cell Biol., *10:* 602–208, 1998.

15. Radinsky, R. Modulation of tumor cell gene expression and phenotype by the organ-specific metastatic environment. Cancer Metastasis Rev., *14:* 323–338, 1995.

16. Gregoire, M., and Lieubeau, B. The role of fibroblasts in tumor behavior. Cancer Metastasis Rev., *14:* 339–350, 1995.

17. Connolly, D. T., Heuvelman, D. M., Nelson, R., Olander, J. V., Eppley, B. L., Delfino, J. J., Siegel, N. R., Leimgruber, R. M., and Feder, J. Tumor vascular permeability factor stimulates endothelial cell growth and angiogenesis. J. Clin. Investig., *84:* 1470–1478, 1989.

18. Sava, G., Clerici, K., Capozzi, I., Gagliardi, R., Cocchietto, M., Alessio, E., Mestroni, G., and Perbellini, A. Reduction of lung metastasis by ImH[*trans*-$RuCl_4$(DMSO)Im]: mechanism of the selective action investigated on mouse tumors. Anticancer Drugs, *10:* 129–138, 1999.

19. Sava, G., Bergamo, A., Zorzet, S., Gava, B., Casarsa, C., Cocchietto, M., Furlani, A., Scarcia, V., Serli, B., Iengo, E., Alessio, E., and Mestroni, G. Influence of chemical stability on the activity of the antimetastasis ruthenium compound NAMI-A. Eur. J. Cancer, *38:* 427–435, 2002.

20. Zorzet, S., Sorc, A., Casarsa, C., Cocchietto, M., and Sava, G. Pharmacological effect of the ruthenium complex NAMI-A given orally to CBA mice with MCa mammary carcinoma. Metal Based Drugs, *8:* 1–7, 2001.

21. Sava, G., Capozzi, I., Clerici, K., Gagliardi, R., Alessio, E., and Mestroni, G. Pharmacological control of lung metastases of solid tumours by a novel ruthenium complex. Clin. Exp. Metastasis, *16:* 371–379, 1998.

22. Albini, A., Iwamoto, Y., Kleinman, K., Matrin, G. R., Aaronson, S. A., Kozlowski, J. M., and McEwan, R. N. A rapid *in vitro* assay for quantitating the invasive potential of tumor cells. Cancer Res., *47:* 3239–3245, 1987.

23. Lockwood, W. R. A reliable and easily sectioned epoxy embedding medium. Anat. Res., *150:* 129–140, 1964.

24. Venable, J. H., and Coggeshall, R. B. A simplified lead citrate stain for use in electron microscope. J. Cell Biol., *25:* 401–408, 1965.

25. Tamura, H., and Arai, T. Determination of ruthenium in biological tissue by graphite furnace AAS after decomposition of the sample by tetramethylammonium hydroxide. Bunseki KagaKu, *41:* 13–17, 1992.

26. Cocchietto, M., Salerno, G., Alessio, E., Mestroni, G., and Sava, G. Fate of the antimetastatic ruthenium complex ImH[*trans*-$RuCl_4$(DMSO)Im] after acute i.v. treatment in mice. Anticancer Res., *20:* 197–202, 2000.

27. Puccetti, P., Romani, L., and Fioretti, M. C. Chemical xenogenization of experimental tumors. Cancer Metastasis Rev., *6:* 93–111, 1987.

28. Ben Efrain, S., Bizzini, B., and Relyveld, E. H. Use of xenogenized (modified) tumor cells for treatment in experimental tumor and human neoplasia. Biomed. Pharmacother., *54:* 268–273, 2000.

29. Sava, G., Salerno, G., Bergamo, A., Cocchietto, M., Gagliardi, R., Alessio, E., and Mestroni, G. Reduction of lung metastases by Na[*trans*-$RuCl_4$(DMSO)Im] is not coupled with the induction of chemical xenogenization. Metal Based Drugs, *3:* 67–73, 1996.

30. Weiss, L. Heterogeneity of cancer cell population and metastasis. Cancer Metastasis Rev., *19:* 351–359, 2000.

31. Magnarin, M., Bergamo, A., Carotenuto, M. E., Zorzet, S., and Sava, G. Increase of tumour infiltrating lymphocytes in mice treated with antimetastatic doses of NAMI-A. Anticancer Res., *20:* 2939–2944, 2000.

32. Garbisa, S., Biggin, S., Cavallarin, N., Sartor, L., Benelli, R., and Albini, A. Tumor invasion: molecular shears blunted by green tea. Nat. Med., *4:* 1216, 1999.

33. Garbisa, S., Sartor, L., Biggin, S., Salvato, B., Benelli, R., and Albini, A. Tumor gelatinases and invasion inhibited by the green tea flavanol epigallocatechin-3-gallate. Cancer (Phila.), *91:* 822–832, 2001.

34. Cocchietto, M., and Sava, G. Blood concentration and toxicity of the antimetastasis agent NAMI-A following repeated intravenous treatment in mice. Pharmacol. Toxicol., *87:* 193–197, 2000.

Clinical Cancer Research

Dual Action of NAMI-A in Inhibition of Solid Tumor Metastasis: Selective Targeting of Metastatic Cells and Binding to Collagen

Gianni Sava, Sonia Zorzet, Claudia Turrin, et al.

Clin Cancer Res 2003;9:1898-1905.